

Influence of a weak external B-field on the plasma parameters and spatial emission profiles of inductively and Helicon-coupled hydrogen discharges

D. Rauner^{1,2}, S. Briefi², P. Gutmann², S. Kurt², U. Fantz^{1,2}

¹Max-Planck-Institut für Plasmaphysik, 85748 Garching, Germany

²AG Experimentelle Plasmaphysik, Universität Augsburg, 86135 Augsburg, Germany

The effect of a weak external B-field on the properties of RF-coupled hydrogen discharges is investigated as it may promise an increased coupling efficiency in comparison to pure inductive coupling. Therefore, plasma parameters of a weakly magnetized ICP are compared to a low-field Helicon discharge using a Nagoya-Type-III antenna. For both setups, the behavior of the electron temperature and density and the density ratio of atomic to molecular hydrogen with varying magnetic field between 0 and 12 mT is presented, as evaluated via optical emission spectroscopy and collisional radiative modelling. The investigations are carried out at a pressure of 1 Pa and a RF-input power of 600 W. Results for the ICP configuration show a steady decrease of all plasma parameters with increasing B-field. In contrast, the low-field-peak occurs with the Helicon setup and the parameters show an increase with increasing B-field. Additionally, radial emission profiles obtained via Abel-inversion are presented, showing the built-up of hollow profiles for both configurations, yet with a different B-field dependency respectively.

1. Introduction

The application of a weak external B-field at low pressure RF-discharges can be beneficial for an increased coupling efficiency. Considerable research of weakly magnetized low pressure plasmas has already been carried out during the last years [1, 2, 3, 4, 5]. Furthermore, the application of Helicon coupling, which relies on wave heating in magnetized cylindrical plasmas, has been the topic of widespread research [6, 7, 8]. It is known for its capability to achieve very high plasma densities at RF-input powers of several kW and at magnetic fields of the order of several 100 mT. However, Helicon discharges can also be operated at lower B-fields, where the so called low-field peak, a local enhancement of the RF-coupling efficiency, is observed.

Both RF-concepts are primarily known for their application in rare gases. However, the investigations presented here are focused on hydrogen plasmas: influenced by a weak external B-field up to 12 mT, discharges are generated at a flexible laboratory experiment, where both a helical ICP-coil and a Nagoya-Type-III antenna for low-field Helicon operation can be applied. Therefore fundamental investigations are carried out as the transition from rare gases to hydrogen is not straightforward: both its nature as a molecular gas and the mass difference compared to rare gases (influencing the magnetization of heavy particles) imply significant differences.

The investigated plasma parameters are obtained via optical emission spectroscopy and collisional radiative models, including the electron temperature and density and the density ratio of atomic to molecular hydrogen. Due to a changing magnetization of charged particles with varying the external B-field, also the spatial plasma profiles are affected. Therefore, radial emission profiles, obtained via Abel-inversion, are evaluated additionally. All results presented were obtained for a pressure of 1 Pa and a RF-input power of 600 W.

2. Experimental Setup

A sketch of the CHARLIE experiment (Concept studies for Helicon Assisted RF Low pressure Ion sourceEs) is shown in figure 1. The continuous wave hydrogen discharge is generated in a cylindrical vessel made of quartz glass, which has a length of 40 cm and a diameter of 10 cm. Operating pressures are in the range between 0.3 and 10 Pa in H₂. The RF-circuit consists of a generator which operates at 13.56 MHz providing a maximum power output of 600 W, the corresponding matchbox and, depending on the current setup, either an ICP coil consisting of 5 helical windings or the Nagoya-Type-III helicon antenna. The external magnetic field, which is orientated parallel to the cylinder axis, is generated via two Helmholtz-coils providing magnetic field strengths up to 12 mT.

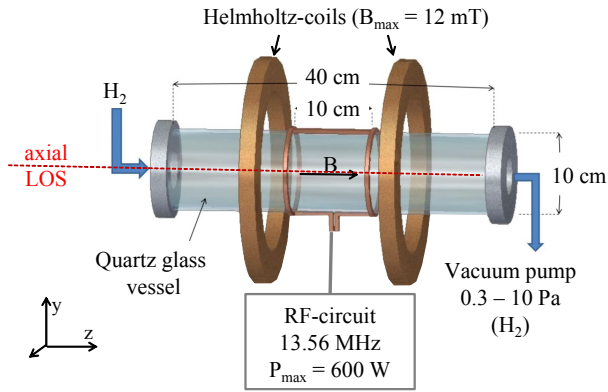


Figure 1: Sketch of the experimental setup. The application of the Nagoya-Type-III helicon antenna is shown exemplarily. Alternatively, a helical ICP-coil (5 windings) can be applied.

3. Diagnostic methods

As diagnostics, optical emission spectroscopy (OES) is applied. Investigations are conducted via an absolutely calibrated high-resolution-spectrometer ($\Delta\lambda_{\text{FWHM}} = 20$ pm) with its line-of-sight equal to the cylinder axis of the vessel. Thereby the absolute emission of the Balmer-series of atomic hydrogen as well as those of the Fulcher transition ($d^3 \Pi_u \rightarrow a^3 \Sigma_g^+$) of molecular hydrogen is measured. Additionally, absolutely calibrated VUV-spectroscopy can be performed at CHARLIE. This is presented as a separate contribution to this conference [9].

Via the application of the collisional radiative models Yacora H [10] for atomic and Yacora H₂ [11] for molecular hydrogen to the spectroscopic measurements, several plasma parameters can be determined subsequently, including the electron temperature T_e and density n_e as well as the ratio of atomic to molecular hydrogen n_H/n_{H_2} . Details and the present status of the CR models are also presented as a contribution to this conference [12].

However, as the plasma parameters are deduced from line-of-sight integrated measurements, changes of the spatial emission profiles of the discharge have to be accounted for separately. Therefore, radial emission profiles $\xi(r)$ are determined from laterally measured intensity profiles $I(y)$ along the cylinder diameter via the application of Abel-inversion:

$$\xi(r) = -\frac{1}{\pi} \int_r^R \frac{dI(y)}{dy} \frac{dy}{\sqrt{y^2 - r^2}}. \quad (1)$$

Due to its singularity, the integral is solved numerically via the Hankel-Fourier-method [13]. All presented profiles were acquired at the central axial position of the vessel for the Helicon configuration or near the center for the ICP setup, as for the latter

the central lateral LOS is blocked due to the coil windings.

4. Results

4.1. Axial emission and plasma parameters

In figure 2, the absolute emission of the H β -line as representative for the atomic radiation and the molecular Fulcher radiation with varying magnetic field is shown as measured along the axial LOS for ICP and Helicon setup. For both configurations a sudden change of the emission occurs when the magnetic field is switched on, leading to an increase for the ICP setup and a decrease for the Helicon setup. For the ICP, this enhancement is caused by a change in the axial plasma distribution, effectively increasing the plasma length along the axial LOS. In Helicon configuration, it is associated with a change of the radial emission profiles, as will be shown in the next section.

In case of the ICP antenna, a further increase of the B-field results in a virtually constant emission up to 3.5 mT and subsequently in a gradual decrease. For the Nagoya-Type-III antenna, a low-field peak of the emission can be observed around 3 to 3.5 mT, followed by a steady increase at higher fields, a behavior which is considered typical for low-field Helicon discharges [14].

In figure 3, the electron temperature and density and the density ratio of atomic to molecular hydrogen gained by the evaluation of the OES measurements are shown. For the ICP configuration, all parameters are decreasing with increasing B-field: T_e is steadily reduced from 4.5 to 2.9 eV, the electron density drops roughly by a factor of two from 1×10^{17} to 5×10^{16} m⁻³ and n_H/n_{H_2} is decreased from 30% at low fields to 10% at higher fields.

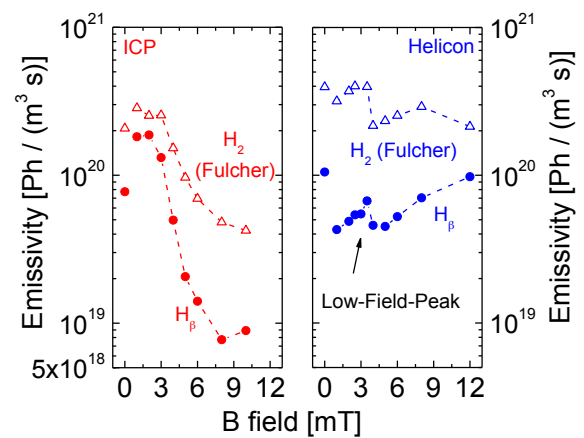


Figure 2: Emissivity of the atomic H β -line and the molecular Fulcher radiation at varying magnetic field for the ICP- and the Helicon-configuration as measured with axial LOS.

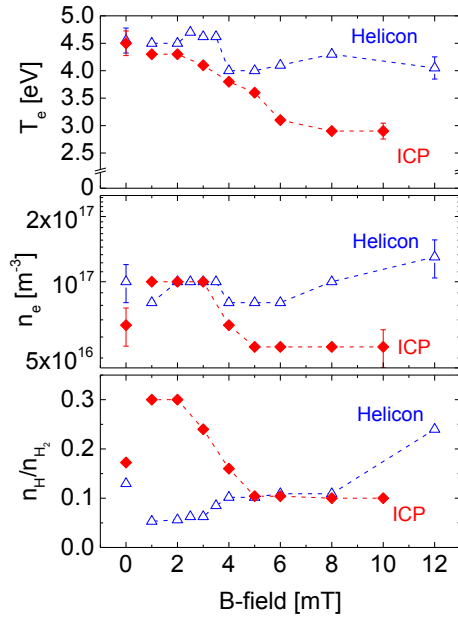


Figure 3: Electron temperature, electron density and density ratio of atomic to molecular hydrogen with varying magnetic field for both ICP- and Helicon-setup.

This behavior is discussed further in the next section, as it can be associated with changes to the radial emission profiles.

In the Helicon setup, both the electron temperature and density are virtually constant within the error margins at values of T_e between 4.0 and 4.5 eV and n_e of about $1 \times 10^{17} m^{-3}$, with the latter being slightly enhanced in the region of the low-field peak and at higher fields. The density ratio of atomic to molecular hydrogen is steadily increasing from 6% up to 24%.

4.2. Radial emission profiles

Exemplarily, the radial profiles of the H_β -emission line of atomic hydrogen are investigated. The radial emission profiles in the ICP configuration for different B-fields are shown in figure 4. Both with the magnetic field switched off and at low fields up to 3.5 mT, a virtually constant emission is observed across the vessel radius with a steep increase of the emission near the vessel walls. At higher fields, the profile changes: for 10 mT the emission near the axis is significantly reduced, leading to a hollow profile with maximal emission near the vessel walls. This can be attributed to the increased magnetization of electrons leading to a reduced heat flux from the skin sheath to the cylinder axis, a mechanism well known from investigations in argon [4]. This also corresponds

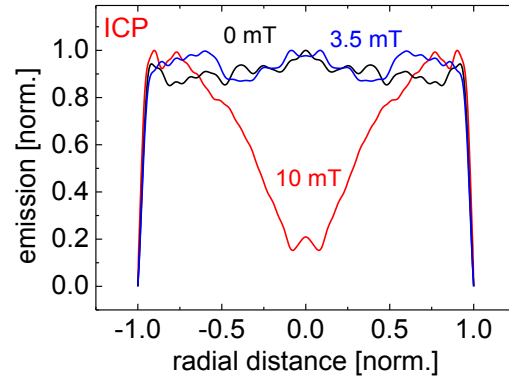


Figure 4: Radial emission profiles of the atomic H_β -line for the ICP-configuration determined via Abel-inversion at different magnetic field strengths.

well with the observed steady decrease of both the axial emission and respectively the plasma parameters at fields above 3.5 mT, as presented in figures 2 and 3.

In figure 5, the radial emission with varying B-field for the Helicon setup is shown. At 0 mT, the profile resembles those of the ICP at low fields, with a virtually constant emission along the radius. However, already at low magnetic fields a change in the radial profiles can be found with the application of the Helicon antenna: again, a transition into hollow profiles with strongly reduced emission along the vessel axis, as it is exemplarily shown for B-fields of 3.5, 5 and 10 mT, is observed. On the one hand, this behavior corresponds well with the sudden decrease of the axial plasma emission when the B-field is switched on, as it is shown in figure 2. On the other hand, the distinct difference compared to the profiles with the ICP-setup indicates a change in the RF-coupling and plasma heating mechanism. To clarify this, spatially resolved measurements of n_e and T_e are planned.

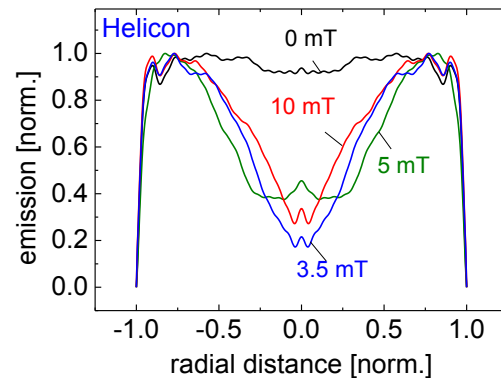


Figure 5: Radial emission profiles of the atomic H_β -line for the Helicon-configuration determined via Abel-inversion at different magnetic field strengths.

4. Conclusion

Hydrogen discharges generated via weakly magnetized inductive and low-field Helicon coupling were investigated regarding the influence of the external magnetic field on the plasma properties. The atomic and molecular emission in the visible range is measured spectroscopically and evaluated via collisional radiative models to obtain the plasma parameters. Additionally, radial emission profiles are acquired via the application of Abel-inversion.

For the ICP configuration, the emission and the plasma parameters show a steady decrease with increasing B-field. At lower fields up to 3.5 mT, the radial emission profiles are virtually constant across the cylinder diameter. At higher fields, a hollow profile is build up, with significantly reduced emission at the cylinder axis.

For the Helicon configuration, the emission shows the typical low-field peak at 3.5 mT, and a general raise with a further increase of the applied B-field. T_e is found to be virtually constant, whereas n_e is only slightly increased at the low-field peak and at higher fields. n_H/n_{H_2} steadily increases with increased B-field. In Helicon configuration, hollow emission profiles are measured already at low B-fields applied, indicating a change of the RF-coupling mechanism compared to the ICP configuration.

5. References

- [1] H. J. Lee et al. *Plasma Sources Sci. Technol.* **5** (1996) 383.
- [2] C. Chung et al. *Phys. Rev. Lett.* **88**(9) (2002) 095002.
- [3] V. A. Godyak, B. M. Alexandrovich, *Phys. Plasmas* **11** (2004) 3553–3560.
- [4] M. Lee, C. Chung, *Phys. Plasmas* **14** (2007) 103507.
- [5] Y. D. Kim et al. *Phys. Plasmas* **20** (2013) 023505.
- [6] F. F. Chen, *Plasma Sources Sci. Technol.* **24** (2015) 014001.
- [7] R. W. Boswell, F. F. Chen *IEEE Transactions on Plasma Science* **25** (1997) 1229–1244.
- [8] F. F. Chen, R. W. Boswell *IEEE Transactions on Plasma Science* **25** (1997) 1245–1257.
- [9] U. Fantz et al. *Proc. of the 32nd ICPIG, Iași* (2015).
- [10] D. Wunderlich et al., *JQSRT* **110** (2009) 62 – 71.
- [11] D. Wunderlich et al., *Proc. of the 30th ICPIG, Belfast* (2011).
- [12] D. Wunderlich et al. *Proc. of the 32nd ICPIG, Iași* (2015).

[13] R. Álvarez et al. *Spectrochim. Acta Part B* **57** (2002), 1665–1680.

[14] F. F. Chen et al., *Plasma Phys. Control. Fusion* **39** (1997) A411–A420.